

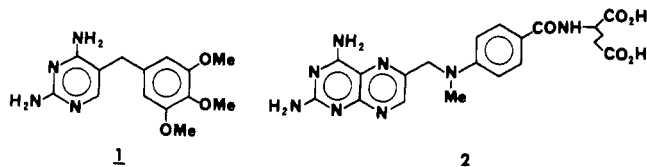
Receptor-Based Design of Dihydrofolate Reductase Inhibitors: Comparison of Crystallographically Determined Enzyme Binding with Enzyme Affinity in a Series of Carboxy-Substituted Trimethoprim Analogues¹

Lee F. Kuyper,^{*,†} Barbara Roth,[†] David P. Baccanari,[†] Robert Ferone,[†] Christopher R. Beddell,[‡] John N. Champness,[‡] David K. Stammers,[‡] John G. Dann,[‡] Frank E. Norrington,[‡] Dorothea J. Baker,[‡] and Peter J. Goodford[‡]

Wellcome Research Laboratories, Burroughs Wellcome Co., Research Triangle Park, North Carolina 27709, and Wellcome Research Laboratories, Langley Court, Beckenham, Kent BR3 3BS, England. Received July 19, 1984

By the use of molecular models of *Escherichia coli* dihydrofolate reductase (DHFR), analogues of trimethoprim (TMP) were designed which incorporated various 3'-carboxyalkoxy moieties in order to acquire ionic interactions with positively charged active-site residues. Certain of these compounds have shown exceptionally high affinity for this enzyme. For example, the 3'-(carboxypentyl)oxy analogue was found to be 55-fold more inhibitory than TMP toward *E. coli* DHFR ($K_i = 0.024$ nM vs. 1.32 nM for TMP). X-ray crystallographic studies of *E. coli* DHFR in binary complexes with TMP and two members of this acid-containing series of compounds defined the binding of these inhibitors and showed the carboxyl group of the latter two inhibitors to be ionically bound to Arg-57. These observations were in agreement with postulated binding modes that were based on receptor modeling.

Dihydrofolate reductase (DHFR) is the primary molecular target of several therapeutically important drugs;² in particular trimethoprim (TMP, 1)³ and methotrexate (MTX, 2)⁴ have found wide use. The enzyme has therefore attracted much attention in the last 20 years.⁵ Recently, X-ray crystallographic studies of DHFR from several sources have yielded three-dimensional molecular structures of the enzyme. Matthews and co-workers have solved structures of the binary complex of *Escherichia coli* DHFR and methotrexate,⁶ of the ternary complex of *Lactobacillus casei* DHFR, NADPH, and MTX,⁷ and of chicken liver DHFR in ternary complex with NADPH and a series of inhibitors including TMP.⁸ Crystallographic refinement of the first two structures has also been reported.⁹ In addition, one of our laboratories has solved the structures of *E. coli* DHFR in binary complex with TMP¹⁰ and with related DHFR inhibitors¹¹ and of L1210 DHFR with NADPH and TMP.¹²



Thousands of DHFR inhibitors have been designed and synthesized over the past three decades, many of them as inhibitors of folate metabolism before the identification of DHFR. Selection of structures for synthesis generally followed the classical approaches of molecular modification.¹³ The availability of the three-dimensional molecular structure of the target enzyme now allows us to augment traditional methodology with mechanistic approaches to inhibitor design. The literature on ligand design based on three-dimensional protein structures is small but growing and is briefly illustrated by the two examples that follow. Beddell and co-workers have reported the successful design of several compounds with affinity for the 2,3-diphosphoglycerate (DPG) binding site of human hemoglobin by the use of wire molecular models of the protein.¹⁴ Not only did they predict the relative oxygen-displacing activities of these compounds with human hemoglobin but they were also able to correlate the activities with structural variations of the DPG binding site found in other hemoglobins.¹⁵ More recently, Blaney et al. were able to

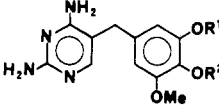
predict the relative binding affinities of four thyroid hormone analogues to prealbumin using computer graphics

- (1) For a preliminary account of this work, see: Kuyper, L. F.; Roth, B.; Baccanari, D. P.; Ferone, R.; Beddell, C. R.; Champness, J. N.; Stammers, D. K.; Dann, J. G.; Norrington, F. E. A.; Baker, D. J.; Goodford, P. J. *J. Med. Chem.* 1982, 25, 1120.
- (2) (a) Roth, B.; Cheng, C. C. In "Progress in Medicinal Chemistry"; Ellis, G. P., West, G. B., Eds.; Elsevier Biomedical Press: Amsterdam, 1982; Vol. 19, p 270. (b) Roth, B.; Bliss, E.; Beddell, C. R. In "Molecular Aspects of Anticancer Drug Action"; Waring, M., Neidel, S., Eds.; Macmillan: London, 1983; p 363.
- (3) (a) Roth, B.; Falco, E. A.; Hitchings, G. H.; Bushby, S. R. M. *J. Med. Pharm. Chem.* 1962, 5, 1103. (b) Bushby, S. R. M.; Hitchings, G. H. *Br. J. Pharmacol. Chemother.* 1968, 33, 72. (c) "Evaluation of New Drugs: Trimethoprim-Sulfamethoxazole"; Finland, M., Kass, E. H., Eds. *J. Infect. Dis.* 1973, 128, Suppl (Nov). (e) "Trimethoprim-Sulfamethoxazole Revisited"; Finland, M., Kass, E. H., Platt, R., Eds. *Rev. Infect. Dis.* 1982, 4, 196-618.
- (4) Livingston, R. B.; Carter, S. K. "Single Agents in Cancer Chemotherapy"; IFI/Plenum: New York, 1970; p 130.
- (5) (a) "Handbook of Experimental Pharmacology"; Hitchings, G. H., Ed.; Springer-Verlag: Berlin, 1983; Vol. 64. (b) Blakley, R. L. *Front. Biol.* 1969, 13. (c) Baker, B. R. "Design of Active-Site Directed Irreversible Enzyme Inhibitors"; Wiley: New York, 1967. (d) McCormack, J. J. *Med. Res. Rev.* 1981, 1, 303. (e) Greaddy, J. E. *Adv. Pharm. Chemother.* 1980, 17, 37.
- (6) Matthews, D. A.; Alden, R. A.; Bolin, J. T.; Freer, S. T.; Hamlin, R.; Xuong, N.; Kraut, J.; Poe, M.; Williams, M.; Hoogsteen, K. *Science* 1977, 197, 452.
- (7) (a) Matthews, D. A.; Alden, R. A.; Bolin, J. T.; Filman, D. J.; Freer, S. T.; Hamlin, R.; Hol, W. G. J.; Kisliuk, R. L.; Pastore, E. J.; Plante, L. T.; Xuong, N.; Kraut, J. *J. Biol. Chem.* 1978, 253, 6946. (b) Matthews, D. A.; Alden, R. A.; Freer, S. T.; Xuong, N.; Kraut, J. *J. Biol. Chem.* 1979, 254, 4144.
- (8) (a) Matthews, D. A.; Volz, K. In "Molecular Structure and Biological Activity"; Griffin, J. F., Daux, W. L., Eds.; Elsevier Biomedical Press: New York, 1982; p 13. (b) Volz, K. W.; Matthews, D. A.; Alden, R. A.; Freer, S. T.; Hansch, C.; Kaufman, B. T.; Kraut, J. *J. Biol. Chem.* 1982, 257, 2528. (c) Matthews, D. A.; Bolin, J. T.; Filman, D. J.; Volz, K. W.; Kraut, J. In "Chemistry and Biology of Pteridines"; Blair, J. A., Ed., de Gruyter: New York, 1983; p 435.
- (9) (a) Bolin, J. T.; Filman, D. J.; Matthews, D. A.; Hamlin, R. C.; Kraut, J. *J. Biol. Chem.* 1982, 257, 13650. (b) Filman, D. J.; Bolin, J. T.; Matthews, D. A.; Kraut, J. *J. Biol. Chem.* 1982, 257, 13663.
- (10) Baker, D. J.; Beddell, C. R.; Champness, J. N.; Goodford, P. J.; Norrington, F. E. A.; Smith, D. R.; Stammers, D. K. *FEBS Lett.* 1981, 126, 49.

[†]Research Triangle Park, NC.

[‡]Kent, England.

Table I. 2,4-Diamino-5-(3,4-disubstituted-5-methoxybenzyl)pyrimidines



no.	R¹	R²	yield, %	recrystn solvent ^b	mp, °C	formula	anal.
3	CH ₂ CO ₂ H	Me	91	A	261–263	C ₁₆ H ₁₈ N ₄ O ₅ ·H ₂ O	C, H, N
4	(CH ₂) ₂ CO ₂ H	Me	12	B	95–125 dec	C ₁₈ H ₂₀ N ₄ O ₅ · ¹ / ₂ H ₂ O	C, H, N
5	(CH ₂) ₃ CO ₂ H	Me	87	B	214–215	C ₁₇ H ₂₂ N ₄ O ₅ · ¹ / ₂ H ₂ O	C, H, N
6	(CH ₂) ₄ CO ₂ H	Me	24	C	183–187	C ₁₈ H ₂₄ N ₄ O ₅ ·HCl	C, H, N, Cl
7	(CH ₂) ₅ CO ₂ H	Me	78	C	182–185	C ₁₉ H ₂₆ N ₄ O ₅ ·HCl	C, H, N, Cl
8	(CH ₂) ₆ CO ₂ H	Me	93	A	148–155	C ₂₀ H ₂₈ N ₄ O ₅	C, H, N
10	Me	(CH ₂) ₃ CO ₂ H	80	A	239–241	C ₁₇ H ₂₂ N ₄ O ₅	C, H, N
11	Me	(CH ₂) ₄ CO ₂ H	75	D	230–232	C ₁₈ H ₂₄ N ₄ O ₅ ·HCl	C, H, N, Cl
13	CH ₂ CO ₂ Me	Me	60	E	206–208	C ₁₆ H ₂₀ N ₄ O ₅ · ¹ / ₅ H ₂ O	C, H, N
14	(CH ₂) ₃ CO ₂ Et	Me	54	F	127–128	C ₁₈ H ₂₄ N ₄ O ₅	C, H, N
15	(CH ₂) ₄ CO ₂ Me	Me	40	F	122–124	C ₁₉ H ₂₆ N ₄ O ₅	C, H, N
16	(CH ₂) ₅ CO ₂ Me	Me	32	F	134–136	C ₂₀ H ₂₈ N ₄ O ₅	C, H, N
17	(CH ₂) ₆ CO ₂ Me	Me	43	G	210–213	C ₂₁ H ₃₀ N ₄ O ₅ ·HCl	C, H, N, Cl
19	Me	(CH ₂) ₃ CO ₂ Et	46	F	138–140	C ₁₉ H ₂₆ N ₄ O ₅	C, H, N
20	Me	(CH ₂) ₄ CO ₂ Me	39	F	147–149	C ₁₉ H ₂₆ N ₄ O ₅	C, H, N

^a Yield of analytically pure product; usually the yield of a single run. ^b A, precipitated from alkali and washed thoroughly with water; B, water; C, methanol/diethyl ether; D, precipitated from alkali, treated with 1 equiv of 1 N HCl, and concentrated to dryness; E, methanol; F, acetone; G, ethanol.

modeling of the thyroxine–prealbumin complex.¹⁶

In this paper we describe the design and synthesis of a series of 3'-carboxyalkoxy analogues of TMP arising from our first attempt at using the DHFR X-ray structures for this purpose. At the time this work began the only *E. coli* DHFR X-ray data available was that of *E. coli* DHFR–MTX. Our goals in this effort were therefore to gain insight into the inhibitor–enzyme interactions for the TMP class of compound and thereby hopefully to provide TMP analogues with higher affinity for *E. coli* DHFR. The compounds resulting from this work showed potent DHFR affinity that was consistent with predictions from molecular modeling, and the postulated binding modes for two of the compounds were verified experimentally by X-ray crystallographic structure determinations of the enzyme–inhibitor complexes.

Results and Discussion

Chemistry. New compounds are listed in Table I. Compounds 13–17 were prepared by alkylation of phenol 22¹⁷ with the appropriate methyl or ethyl ω-bromoalkanoate with use of potassium *tert*-butoxide in Me₂SO. Subsequent basic hydrolysis with sodium hydroxide in methanol/water gave the corresponding carboxylic acids, compounds 3 and 5–8. Analogous procedures were employed for the preparation of esters 18–21 and acids 9–12 from phenol 23.¹⁸ Attempts to alkylate compounds 22 and 23 with methyl 3-bromopropionate failed, presumably because of competing elimination reactions. This problem

was circumvented by the use of 3-bromopropionic acid for alkylation of phenol 22 which gave compound 4 directly. The same strategy was not successful for the alkylation of phenol 23; the para-substituted analogue of 4 was therefore not prepared. Compounds 9, 12, 18, and 21 in Table II have been previously reported.¹⁹

Inhibitor Design. In the *unrefined* model of the *E. coli* DHFR–MTX complex originally available to us, the α-carboxy group of the inhibitor forms an ionic linkage to the guanidinium moiety of Arg-57, and the γ-carboxy group apparently interacts with the aminoalkyl side chain of Lys-32. The association of MTX with two basic residues of *E. coli* DHFR and the presence of a third positively charged residue, Arg-52, near the binding cleft suggested to us that analogues of TMP containing appropriately placed carboxylic acid substituents might interact with one or more of these positively charged sites. The consequence might be to increase affinity for the enzyme and possibly give information about the binding of TMP itself. Compound 7 was prepared on the basis of that premise, following a preliminary fitting of some potential analogue structures to the enzyme model. Affinity data from 7 for *E. coli* DHFR is shown in Table II. The exceptionally low value of *K_i* observed for compound 7 suggested that the desired ionic interaction with the enzyme did occur and led us to consider the three potential sites for that interaction, namely, Lys-32, Arg-52, and Arg-57, in more detail.

In crystalline *E. coli* DHFR–MTX there are two independent complexes in the crystallographic asymmetric unit. The α-carboxy group of MTX is clearly associated with Arg-57 in both complexes. In the *unrefined* model only one of the two complexes showed a possible interaction between Lys-32 and the γ-carboxy group of MTX, suggesting this particular association to be a weak one. In the recently reported refined structure of *E. coli* DHFR–MTX the γ-carboxylate of MTX is modeled in the same manner in each of the two independent complexes. It does not hydrogen bond directly to Lys-32 or to any other protein residue but interacts with several water molecules that in turn are hydrogen bonded to Lys-32 and to the α-carboxylate and benzoylcarbonyl oxygen of MTX.⁹ The

- (11) Baker, D. J.; Beddell, C. R.; Champness, J. N.; Goodford, P. J.; Norrington, F. E. A.; Roth, B.; Stammers, D. K. *Acta Crystallogr., Sect. A* 1981, A37 (Suppl), C-58.
- (12) Stammers, D. K.; Champness, J. N.; Dann, J. G.; Beddell, C. R. In "Chemistry and Biology of Pteridines"; Blair, J. A., Ed.; de Gruyter: New York, 1983; p 567.
- (13) Blaney, J. M.; Hansch, C.; Silipo, C.; Vittoria, A. *Chem. Rev.* 1984, 84, 333.
- (14) Beddell, C. R.; Goodford, P. J.; Norrington, F. E.; Wilkinson, S.; Wootton, R. *Br. J. Pharmacol.* 1976, 57, 201.
- (15) Beddell, C. R.; Goodford, P. J.; Stammers, D. K.; Wootton, R. *Br. J. Pharmacol.* 1979, 65, 535.
- (16) Blaney, J. M.; Jorgensen, E. C.; Connolly, M. L.; Ferrin, T. E.; Langridge, R.; Oatley, S. J.; Burridge, J. M.; Blake, C. C. F. *J. Med. Chem.* 1982, 25, 785.
- (17) Rey-Bellet, G.; Reiner, R. *Helv. Chim. Acta* 1970, 53, 945.
- (18) Brossi, A.; Grunberg, E.; Hoffer, M.; Teitel, S. *J. Med. Chem.* 1971, 14, 58.

- (19) Roth, B.; Aig, E.; Rauckman, B. S.; Strelitz, J. Z.; Phillips, A. P.; Ferone, R.; Bushby, S. R. M.; Sigel, C. *J. Med. Chem.* 1981, 24, 933.

Table II. Affinity Data from Compounds 1, 3–21, and *E. coli*, Rat Liver, and Chicken Liver DHFRs

no.	R ¹	R ²	<i>E. coli</i>		rat liver:	chicken liver:
			rel binary K _D ^a	10 ³ K _i ^b M	10 ⁴ I ₅₀ , M	10 ⁴ I ₅₀ , M
1 (TMP)	Me	Me	1.0	1.3	3.4	7.5
3	CH ₂ CO ₂ H	Me	1.2	2.6	0.70	
4	(CH ₂) ₂ CO ₂ H	Me	0.29	0.37	0.74	
5	(CH ₂) ₃ CO ₂ H	Me	0.15	0.035	0.097	0.22
6	(CH ₂) ₄ CO ₂ H	Me	0.13	0.066	0.27	
7	(CH ₂) ₅ CO ₂ H	Me	0.063	0.024	0.35	
8	(CH ₂) ₆ CO ₂ H	Me	0.13	0.050	0.56	
9	Me	CH ₂ CO ₂ H		16.	20% @ 2.2	
10	Me	(CH ₂) ₃ CO ₂ H		5.2	4.0	3.5
11	Me	(CH ₂) ₄ CO ₂ H		2.2	6.4	
12	Me	(CH ₂) ₅ CO ₂ H		3.1	3.0	
13	CH ₂ CO ₂ Me	Me		11.	15% @ 0.42	
14	(CH ₂) ₃ CO ₂ Et	Me		0.47	1.6	
15	(CH ₂) ₄ CO ₂ Me	Me		0.76	1.3	
16	(CH ₂) ₅ CO ₂ Me	Me		0.86	1.8	
17	(CH ₂) ₆ CO ₂ Me	Me		1.9	1.1	
18	Me	CH ₂ CO ₂ Et		2.7	12% @ 4.0	
19	Me	(CH ₂) ₃ CO ₂ Et		2.3	17% @ 0.9	
20	Me	(CH ₂) ₄ CO ₂ Me		4.1	0% @ 1.0	
21	Me	(CH ₂) ₅ CO ₂ Me		9.8	11.0	

^a Relative K_D values are normalized to the value of TMP such that a value less than 1 indicates higher affinity than that of TMP. Values of multiple determinations agreed within ±20%. ^b K_i values for compounds 1 and 3–8 were measured directly and those for compounds 9–21 were calculated from I₅₀ values. See the Experimental Section for additional details. For each method, values of multiple determinations agreed within ±15%.

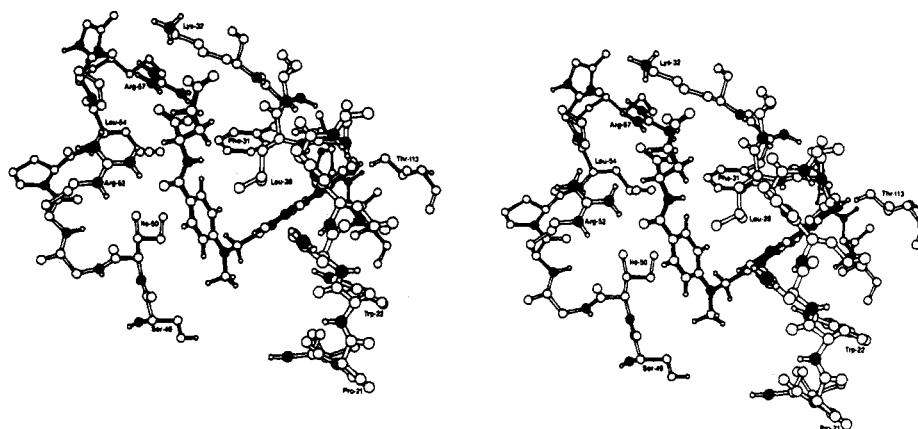


Figure 1. A stereo drawing of the methotrexate binding site of *E. coli* DHFR. Methotrexate is indicated by solid bonds and protein by open bonds. Hydrogen atoms are represented by the small circles and are included on all appropriate atoms of methotrexate but only on nitrogen and oxygen atoms of the protein. Nitrogen atoms are indicated by blackened circles. Selected amino acid residues are labeled.

active-site region of this refined structure, with water molecules omitted, is illustrated in Figure 1.

The Arg-57 residue of *E. coli* DHFR is strictly conserved in all normal DHFRs that have been sequenced.^{8b,21} Lysine-32, a nonconserved residue, exists only in the *E. coli* enzyme. However, all other normal DHFRs contain a basic residue at a position corresponding to 29 and/or 33 in *E. coli* DHFR, and side chains at these positions can conceivably substitute spatially for Lys-32. In the X-ray structure of MTX in ternary complex with *L. casei* DHFR and NADPH, the α -carboxy group interacts with the Arg

residue of *L. casei* DHFR that is structurally equivalent to Arg-57 of the *E. coli* enzyme. The γ -carboxy group is associated with His-28, a residue corresponding to Ala-29 in *E. coli* DHFR. This latter interaction also appears to be a weak one, as indicated by the apparent disorder of the γ -carboxylate side chain observed in the refined structure.⁹ Volz et al.^{8b} have shown that DHFR from chicken liver is structurally similar to the *E. coli* and *L. casei* enzymes and have identified Arg-70 of the enzyme from chicken liver to be structurally equivalent to Arg-57 of *E. coli* DHFR.

Binding studies of Piper and co-workers²² are in accord with this structural information. These workers have

- (20) Unrefined atomic coordinates for the complex between *E. coli* DHFR and MTX, generously provided by Drs. D. Matthews and J. Kraut (ref 6), were used in the construction of Kendrew wire models.
- (21) Hitchings, G. H.; Smith, S. L. In "Advances in Enzyme Regulation"; Weber, G., Ed.; Pergamon: New York, 1980; Vol. 18, p 349.

- (22) (a) Piper, J. R.; Montgomery, J. A. In "Chemistry and Biology of Pteridines"; Kisliuk, R. L., Brown, G. M., Eds.; Elsevier/North Holland: New York, 1979; p 261. (b) Piper, J. R.; Montgomery, J. A.; Sirotinak, F. M.; Chello, P. L. *J. Med. Chem.* 1982, 25, 182.

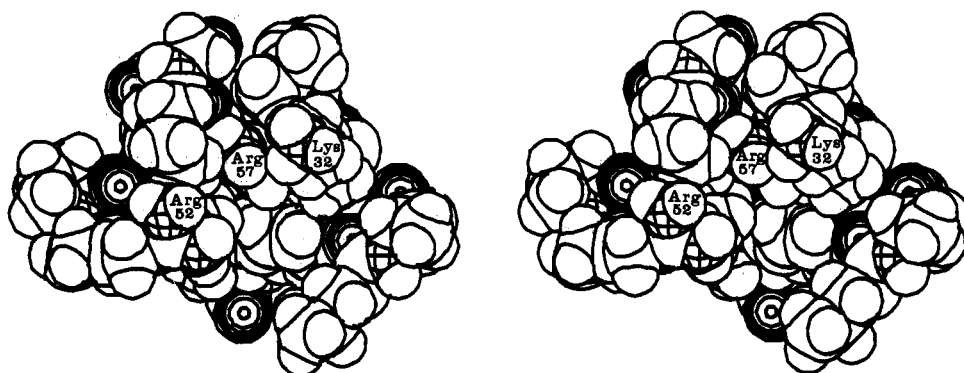


Figure 2. A stereo space-filling representation of the *E. coli* DHFR binding site for the glutamate portion of methotrexate. Atom labeling is as follows: carbon and hydrogen, open; nitrogen, crosshatched; oxygen, concentric circles.

prepared the α - and γ -monoamides of MTX and have found that the former derivative shows a considerably weaker inhibition than that of MTX for DHFR from pigeon liver and from L1210 cells. In contrast, the γ -monoamide is essentially equivalent to MTX in its inhibition of these two enzymes, presumably indicating the greater importance to enzyme binding of the α -carboxy group of MTX. The high sequence homology (76%) between DHFR from L1210 cells and that from chicken liver strongly suggests that the structure of L1210 DHFR is correspondingly similar. The sequence of DHFR from pigeon liver has not been reported.

As illustrated in Figure 2, the local molecular environment of Arg-57 is quite different from that of Lys-32 and Arg-52. The side chain of Arg-57 is significantly buried in a hydrophobic region, with the guanidinium moiety flanked by Phe-31, Leu-36, Val-40, Leu-54, and Pro-55. In contrast, the side chains of Lys-32 and Arg-52 lie at the enzyme surface, extended into the solvent. The dielectric constant in the hydrophobic environment surrounding Arg-57 will be lower than that in bulk solvent and should enhance ionic interactions.²³

The points discussed above implicated Arg-57 as the binding site for the carboxy group of compound 7. Molecular modeling experiments fitting TMP into the active site of *E. coli* DHFR were consistent with that idea. With the pyrimidine ring of TMP positioned in the active site of DHFR in a manner identical with that of MTX, the conformation of TMP was adjusted to match that of its crystalline hydrobromide salt.²⁴ Roth et al. suggested this particular conformation as the active one on the basis of DHFR affinity for a series of 6-substituted analogues of TMP.²⁵ In this conformation the phenyl ring of TMP was oriented in the active site somewhat similar to that of MTX and appeared to fit sterically. One of the *m*-methoxy groups was disposed directly toward the guanidinium moiety of Arg-57, and the (carboxypentyl)oxy chain of compound 7 could be modeled at that position for an optimal interaction (two approximately parallel hydrogen bonds²⁶) with the guanidinium group of Arg-57. Similar modeling of shorter carboxyalkoxy substituents suggested that the chain lengths of one and two methylene units

might be too short for such an interaction, although the crudeness of our modeling experiments limited our confidence in such predictions. However, as discussed below, subsequent synthesis and DHFR affinity measurements of the remaining compounds in this series produced results that were compatible with these modeling postulates.

Enzyme Affinity. Kinetic K_i and equilibrium K_D affinity data for *E. coli* DHFR are presented in Table II, along with I_{50} data for rat liver and chicken liver DHFRs. As is evident from Table II, compounds 5–8 are exceptionally active inhibitors of *E. coli* DHFR. The K_i of compound 7 is 55-fold lower than that of TMP and is comparable to the K_i measured for MTX (MTX K_i = 0.021 nM).²⁷ The relative activity profile from the equilibrium K_D data is very similar to that from the K_i results. The significantly higher affinity of acids 5–8, compared with that of TMP and the corresponding esters 10–13, indicated the importance of the carboxy group and implied that the desired ionic interaction did occur for these carboxy-containing compounds. In addition, the weaker affinity of the shorter chain acids 3 and 4 agreed well with our modeling predictions and supported the assignment of Arg-57 as the site of interaction for the carboxy group.

X-ray Crystal Structures. As mentioned in the introduction, the X-ray structure of TMP in complex with *E. coli* DHFR has been reported.¹⁰ We present here the structures of *E. coli* DHFR complexed with the carboxy-containing compounds 4 and 7. In the discussion that follows these structures will be described and related to the observed inhibitor–enzyme affinity constants presented in Table II.

It should first be emphasized that the *E. coli* DHFR structures discussed here are binary complexes of enzyme and inhibitor: the cofactor NADPH is not present. Therefore the most meaningful comparison of affinity to the enzyme–inhibitor structures at hand will rely on the relative binary K_D values in Table II. The kinetic K_i constants are by necessity a measure of affinity in the ternary complex. The cooperative effect of NADPH and TMP on affinity has been well documented²⁸ and suggests the possibility that the binary and ternary complexes may differ somewhat in enzyme conformation and/or the mode of binding of TMP. Any interpretation of K_i data in terms of the three-dimensional enzyme structures presented here involves the assumption that structural differences between the binary and ternary complexes are too small to modify profiles of relative activity, even though they may modify absolute values of affinity.

(23) (a) Weber, G. *Adv. Protein Chem.* 1975, 29, 1. (b) Epstein, H. *J. Theor. Biol.* 1971, 31, 69. (c) Barlow, D. J.; Thornton, J. M. *J. Mol. Biol.* 1983, 168, 867.

(24) Phillips, T.; Bryan, R. F. *Acta Crystallogr., Sect. A* 1969, A25, S200.

(25) Roth, B.; Aig, E.; Lane, K.; Rauckman, B. S. *J. Med. Chem.* 1980, 23, 535.

(26) (a) Salunke, D. M.; Vizayan, M. *Int. J. Peptide Protein Res.* 1981, 18, 348. (b) Nakagawa, S.; Umeyama, H. *J. Am. Chem. Soc.* 1978, 100, 7716.

(27) Baccanari, D. P.; Joyner, S. S. *Biochemistry* 1981, 20, 1710.

(28) Baccanari, D. P.; Daluge, S.; King, R. W. *Biochemistry* 1982, 21, 5068.

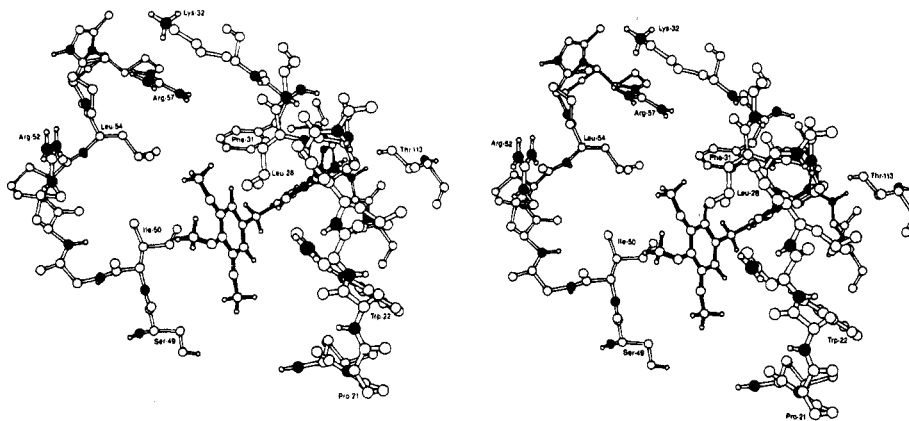


Figure 3. A stereo drawing of the trimethoprim binding site of *E. coli* DHFR. Trimethoprim is indicated by solid bonds and protein by open bonds. Hydrogen atoms are represented by the small circles and are included on all appropriate atoms of trimethoprim but only on nitrogen and oxygen atoms of the protein. Nitrogen atoms are indicated by blackened circles. Selected amino acid residues are labeled.

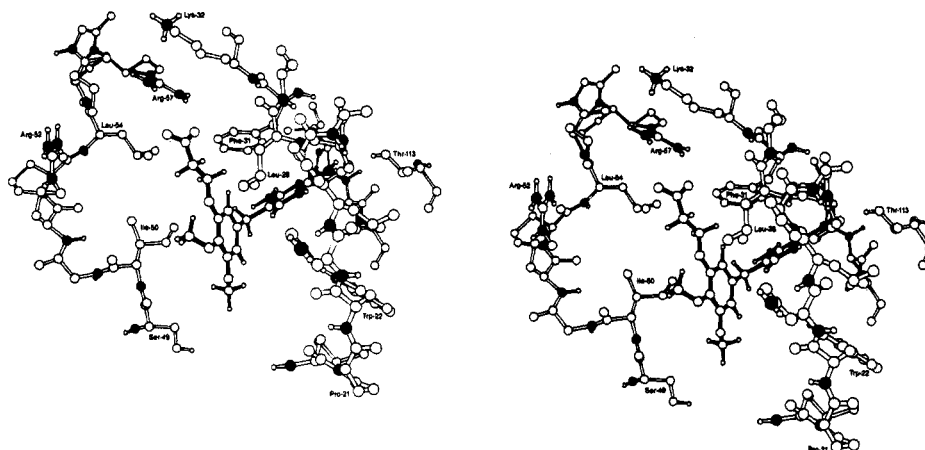


Figure 4. A stereo drawing of the binding site for compound 4 in *E. coli* DHFR. Compound 4 is indicated by solid bonds and protein by open bonds.

The *E. coli* DHFR-TMP X-ray structure shows that TMP binds in a manner very similar to that suggested by our early simple molecular modeling experiments. As in the *E. coli* DHFR-MTX crystals, the crystallographic asymmetric unit of *E. coli* DHFR-TMP contains two independent enzyme-inhibitor complexes. One of these complexes is shown in Figure 3.²⁹ The binding of TMP is similar in the two complexes; the protonated pyrimidine ring of TMP is ionically associated with Asp-27, analogous to the interaction observed for MTX, and the trimethoxyphenyl ring is directed outward from the enzyme cleft with the ring plane roughly aligned with the cleft. As postulated above, the conformation of TMP in the enzyme complex is very similar to that observed for the hydrobromide salt of TMP in the crystal and closely matches one of the two postulated binding modes proposed by Roberts and co-workers based on elegant NMR studies of TMP in solution with the *E. coli* and *L. casei* enzymes.³⁰

In the crystalline complex the 3'-methoxy group of TMP is positioned close to the side chains of Leu-28 and Leu-54, as well as the edge of the ring of Phe-31, and this methoxy group projects directly toward the guanidinium group of Arg-57. The 4'-methoxy group is located near Ile-50 at the edge of the cleft, and the 5'-methoxy group is isolated in the open, lower part of the cleft. By analogy with the *L. casei* DHFR-MTX-NADPH structure,⁹ this open part of the cleft in the binary complex is almost certainly occupied by NADPH in the ternary complex. Baccanari et al. have speculated that direct interaction between the 5'-methoxy group of TMP and the cofactor may be in part responsible for the observed cooperativity of the two ligands.²⁸

The potential interaction between Arg-57 and the carboxy groups of compounds 4 and 7 was confirmed by the corresponding enzyme-inhibitor X-ray structures. The mode of binding for the diaminopyrimidine portion of compounds 4 and 7 appears to be essentially the same as that of TMP, as indicated by the featureless nature of the corresponding regions in the difference electron density maps (see Experimental Section). The combined maps of the two complexes showed a slight difference in the location of the benzyl portion of each. Whereas they appear to locate in almost identical planes, the benzyl group of compound 7 is shifted in plane about 0.5 Å related to compound 4, away from the Arg-57 side chain. Significant positive electron density was observed between the side chain of Arg-57 and what corresponds to the 3'-methoxy group of TMP in both sets of difference maps. This electron density was seen very clearly for both molecules

- (29) Figure 3 was drawn with use of refined atomic coordinates of the *E. coli* DHFR-TMP complex generously provided by D. A. Matthews et al. (unpublished results). These coordinates were also used for the protein portion of the structures shown in Figures 4 and 5. It should be noted that the only major difference in protein structure between the *E. coli* DHFR-TMP complex and the corresponding enzyme complex with MTX is the conformation of the Arg-52 side chain.
- (30) (a) Cayley, P. J.; Albrand, J. P.; Feeney, J.; Roberts, G. C. K.; Piper, E. A.; Burgen, A. S. V. *Biochemistry* 1979, 18, 3887. (b) Birdsall, B.; Roberts, G. C. K.; Feeney, J.; Dann, J. G.; Burgen, A. S. V. *Biochemistry* 1983, 22, 5597.

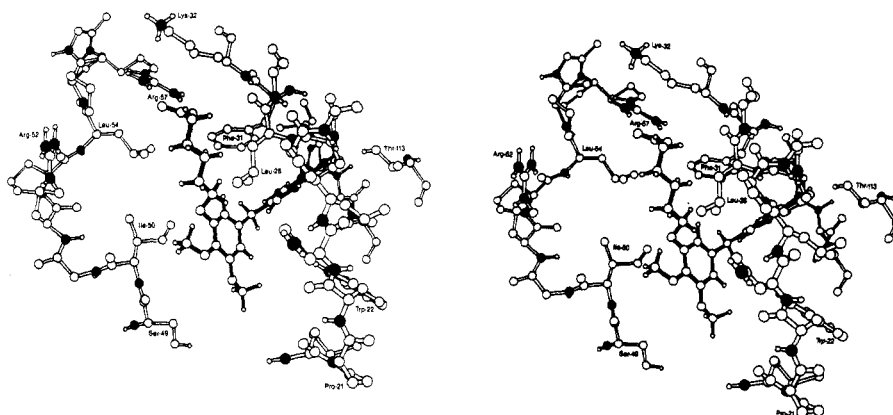


Figure 5. A stereo drawing of the binding site for compound 7 in *E. coli* DHFR. Compound 7 is indicated by solid bonds and protein by open bonds.

of the complex within the asymmetric unit, in difference and in combined maps. In the former maps, the density was generally above about 3 times the estimated root mean square error for the density and two- to threefold higher still near the carboxy group. Density from the carboxy group of 7 was clearly closer to the guanidinium moiety of Arg-57 than that of 4. Results of modeling to the densities are illustrated in Figures 4 and 5. Modeling of compound 4 was compatible with the existence of a single hydrogen bond between its carboxy moiety and the guanidinium group of Arg-57, whereas the corresponding interaction with compound 7 accommodated two approximately parallel hydrogen bonds. The resolution of the density did not unambiguously define the conformation of the alkoxy linkage of 7, but the conformation shown in Figure 5 provided a reasonable fit to the electron density.

These structural observations agreed well with the differences in observed enzyme affinity for TMP and compounds 4 and 7. Although the exact nature of the effect of chain length on affinity for compounds 3–8 is not understood, one can conclude that if the chain length is sufficiently long to allow two hydrogen bonds between the carboxy and guanidinium groups, then high affinity is observed. The conformational energy and various contacts with the enzyme of the side chain must contribute to the observed affinity of compounds 3–8, but the Arg-57 interaction appears to be the dominant factor. It is interesting to note that simple modeling studies indicate that the carboxyalkoxy chain of compound 7 can be altered to reach the amino group of Lys-32 or the guanidinium group of Arg-52 with no obvious conformational or steric problems. The observed association with Arg-57 is evidence for the postulated effect of a hydrophobic environment on the attraction of the guanidinium moiety with the carboxy-substituted side chains of the inhibitor.

Modeling of the 4'-carboxyalkoxy inhibitors, compounds 9–12, suggested a possible ionic interaction with the guanidinium group of Arg-52 on the enzyme surface. This particular association would be expected to be weak because of the substantial exposure to solvent. Indeed the K_i values of acids 9–12 are all higher than that of TMP and are essentially equivalent to those of the corresponding esters, compounds 18–21, with one exception. The short-chain acid 9 is a substantially weaker binder than its corresponding ester 18 and TMP. These affinity data are consistent with the surface location of the 4'-position of TMP in the binary *E. coli* DHFR complex. Previous work has also deduced the solvent-accessible nature of the 4'-position of TMP, on the basis of the affinities of a variety of substituents.¹⁹ The poor affinity of 9 has been rationalized in terms of close contact between enzyme and

carboxy substituent and the resultant desolvation of the polar carboxy group. Molecular modeling lends support for this idea.

The relative inhibitory activity profile of compounds 1 and 3–21 with rat liver DHFR is very similar to that observed with the *E. coli* enzyme. As mentioned in the introduction, the X-ray structures of TMP in ternary complex with chicken liver DHFR^{8c} and with L1210 DHFR¹² have recently been solved, and it is tempting to try to use such information to rationalize the rat liver DHFR inhibition data. Although the amino acid sequence of the rat liver enzyme is not known, the high sequence homology among enzymes from chicken, mouse, cow, pig, and human sources suggests that the rat enzyme will also have similar primary and tertiary structure.^{8b,21} The activities of compounds 5 and 10 relative to that of TMP against rat liver DHFR are indeed similar to those measured against chicken liver DHFR.

Modeling of the acid-containing analogues to the chicken enzyme structure, using a Kendrew model of the TMP complex³¹ and assuming that the analogues have the conformation adopted by TMP with this enzyme, did not provide a straightforward rationalization of the observed affinities. The conformation of TMP in its complex with chicken liver DHFR is very different from that observed in its complex with the *E. coli* enzyme.^{8c} One *m*-methoxy group of TMP is buried in a hydrophobic pocket near Val-115 and is "walled off" from Arg-70 (homologous with Arg-57 of *E. coli* DHFR) by the side chains of Phe-34 and Leu-67. It appears sterically impossible to substitute that methoxy group with any of the carboxyalkoxy groups. The other meta position is at the enzyme surface and relatively open to substitution, but carboxyalkoxy groups there cannot reach the guanidinium ion of Arg-70. Interaction of an acidic substituent at this latter meta position with Arg-28 or Lys-32 could conceivably occur, but side chains of these residues are on the enzyme surface and, as argued above in the discussion of *E. coli* DHFR, such solvent-exposed cations would not be expected to interact strongly with anions.

Alternatively, it seems possible that the meta-acid analogues might adopt a conformation when bound to chicken liver DHFR that is similar to the conformation of TMP and compounds 4 and 7 in their *E. coli* DHFR complexes. This would allow the inhibitor's carboxy group to interact with Arg-70 of chicken DHFR, in analogy with the *E. coli* DHFR mode of binding. Assessment of this

(31) Refined atomic coordinates for the complex between chicken liver DHFR, NADPH, and TMP were provided by Drs. D. Matthews and J. Kraut (ref 8).

conformational possibility was difficult to make with use of Kendrew models, but it appeared to be sterically reasonable.

Modeling of the *p*-carboxyalkoxy analogues to chicken DHFR also gave less than satisfactory results. In the chicken liver DHFR-TMP structure the *p*-methoxy group of TMP is located in a position resembling that of the 3'-methoxy of TMP in its complex with *E. coli* DHFR. This suggests that carboxyalkoxy groups in the para position of TMP might be able to bind to Arg-70 and thereby enhance affinity to chicken liver DHFR. As shown in Table II this did not occur. Perhaps subtle steric or conformational factors offset any affinity associated with the postulated carboxy-Arg-70 interaction. Again, Kendrew models seem inadequate to assess such subtleties. We hope to address these questions experimentally with X-ray crystal structures of appropriate enzyme-inhibitor complexes.

In Vitro Antibacterial Activity. Data from representative organisms are shown in Table III. In general, compounds in this series displayed moderate-to-good activity against Gram-positive organisms. For example, the most active DHFR inhibitors in this series, compounds 6-8, showed activities against *S. aureus* that were essentially equivalent to that of TMP. Relatively weak activity was observed for these compounds against Gram-negative organisms. The only analogue in this series that showed activity comparable to that of TMP against the Gram-negative organisms *E. coli* and *Sal. typhosa* was compound 4. The potential decomposition of 4 via a retro-Michael reaction to give the corresponding phenol and acrylic acid might be involved in its unique activity, but we have not studied this compound in depth to examine this possibility. The activity of the postulated product phenol 22 is very similar to that of 4 against these two organisms.

For those compounds containing carboxy groups, poor activity might be at least partly ascribed to the acidic functionality and its reputed association with problems in penetration of the bacteria.³² The relative inactivity of the esters, however, suggests that acidity is not the only factor involved.

Conclusion

Three-dimensional molecular models of the *E. coli* DHFR-MTX complex were used to design analogues of TMP that show up to 55-fold higher affinity for the enzyme than does TMP. The predicted mode of binding was confirmed by X-ray crystallographic studies of TMP and two of these analogues in complex with *E. coli* DHFR. However, the simple modeling procedures used for this successful effort in inhibitor design were inadequate to rationalize the affinity of chicken liver DHFR for the same series of inhibitors, indicating a need for more rigorous modeling techniques as well as additional X-ray crystallographic work. Nonetheless, these results clearly demonstrate the usefulness of enzyme molecular modeling as a tool for inhibitor design.

Experimental Section

Chemistry. Melting points were determined in open capillaries on a Thomas-Hoover apparatus and are uncorrected. Elemental analyses were performed by Dr. Stuart Hurlbert and staff of Burroughs Wellcome Co. or by Atlantic Microlab, Inc., Atlanta, GA. Where indicated by symbols of the elements, the analytical results obtained were within 0.4% of the calculated values. The spectroscopic data for all new compounds were consistent with

the assigned structures. The NMR spectra were determined by Dr. S. Hurlbert and his staff and were recorded on a Varian XL-100 or CFT-20 spectrometer in Me₂SO-*d*₆. UV spectra were determined on a Cary 118 spectrophotometer.

General Procedure for Alkylation of Compounds 22 and 23. To a solution of compound 22 or 23 (1-30 mmol) in Me₂SO (5 mL/mmol of phenol) was added 1.1 equiv of *t*-BuOK with stirring under a N₂ atmosphere. The solution was stirred at room temperature for 0.25-0.5 h. Occasionally, a white precipitate would form during this time. To this solution or suspension was added 1.1 equiv of a methyl or ethyl ω -bromoalkanoate, and the homogeneous solution was stirred at room temperature. The reaction was monitored by TLC on silica gel with CH₂Cl₂:CH₃OH (4:1). When it was considered complete, generally within 2 h, solvent was removed at reduced pressure and the residual brown oil was subjected to column chromatography on silica gel, eluting with 1-5% MeOH in CH₂Cl₂. Those fractions containing the desired product were pooled and concentrated to dryness. The solid was then recrystallized from an appropriate solvent such as methanol, ethanol, or acetone.

General Procedure for Hydrolysis of Esters 13-20. To a solution or suspension of the ester (1-5 mmol) in MeOH (~5 mL/mmol of ester) was added 3.0 equiv of 1.0 N NaOH. The mixture was stirred at room temperature and monitored by TLC. When ester was no longer detectable, the solution was neutralized with 3.0 equiv of 1.0 N HCl. This generally caused precipitation of a white solid which was washed with or recrystallized from water. In some instances the product precipitated from the neutralized reaction mixture as the partial hydrochloride salt, in which case it was converted entirely to that salt with 1 N HCl.

2,4-Diamino-5-[3-(carboxyethoxy)-4,5-dimethoxybenzyl]-pyrimidine (4). To a solution of 2.76 g (10.0 mmol) of phenol 22 in 25 mL of Me₂SO was added 2.4 g (21 mmol) of *t*-BuOK. This mixture was stirred at room temperature for about 10 min to give a homogeneous tan solution. To this was added in one portion 1.60 g (10.5 mmol) of 3-bromopropionic acid and the solution was stirred at room temperature for 20 h. Solvent was removed at reduced pressure and the residue was taken up in 20 mL of water. Upon storage overnight 1.27 g of starting phenol 22 precipitated as a white crystalline solid and was removed by filtration. To the aqueous filtrate was added 0.8 mL (10 mmol) of concentrated HCl. The tan precipitate that soon formed was filtered and recrystallized from water to give 0.72 g of a white fluffy solid which was identified as the partial hydrochloride salt of the desired product. The compound was suspended in 20 mL water and treated with 0.19 mL (2.2 mmol) of concentrated hydrochloric acid to give a homogeneous solution. Solvent was removed at reduced pressure, the residue was taken up in 20 mL of absolute ethanol, and 200 mL of anhydrous ether was added to produce a white precipitate. The solid was filtered and dried to yield 0.68 g of a white powder, mp 105-150 °C dec (softened 95 °C), which analyzed as the half hydrate of the hydrochloride salt of 4 (anal. C₁₆H₂₁ClN₄O₅·1/2H₂O: C, H, N, Cl). This salt was converted to the free base with 1 equiv of 1.0 N NaOH. The resulting solid was recrystallized from water to give an off-white powder: mp 95-125 °C dec; UV (0.1 N HCl) max 203 nm (ϵ 58400), 270 (ϵ 6100); NMR (Me₂SO-*d*₆) δ 2.65 (t, 2, CH₂, *J* = 6 Hz), 3.53 (s, 2, CH₂), 3.60 (s, 3, OMe), 3.72 (s, 3, OMe), 4.12 (t, 2, CH₂, *J* = 6 Hz), 6.10 (br s, 2, NH₂), 6.34 (br s, 2, NH₂), 6.57 (s, 2, *o*-H's), 7.51 (s, 1, pyrimidine C6-H).

Biological Assays. *E. coli* DHFR was the homogeneous form one isozyme from strain RT 500.³³ The rat liver enzyme was either partially purified or purified to homogeneity: kinetic results from these two preparations were identical. Homogeneous enzyme was prepared by mixing the Sephadex G-100 pool³⁴ overnight with Methotrexate-Sepharose resin³⁵ (1 mL of resin/10 units of enzyme). The enzyme-bound resin was poured into a column and extraneous protein was removed by washing with 50 mM potassium phosphate buffer, pH 8, 1 mM EDTA, 0.5 M KCl. Dihydrofolate reductase was specifically eluted by the addition of

(32) (a) Bellomo, P.; Marchi, E.; Mascellani, G.; Brufani, M. *J. Med. Chem.* 1981, 24, 1310. (b) Davis, B. D. *Arch. Biochem. Biophys.* 1958, 78, 497.

(33) Baccanari, D. P.; Stone, D.; Kuyper, L. F. *J. Biol. Chem.* 1981, 256, 1738.

(34) Burchall, J. J.; Hitchings, G. H. *Mol. Pharmacol.* 1965, 1, 126.

(35) Baccanari, D. P.; Phillips, A.; Smith, S.; Sinski, D.; Burchall, J. J. *Biochemistry* 1975, 14, 5265.

Table III. Relative in Vitro Antibacterial Activity of Compounds 1, 3–9, 12–18, and 21 against Selected Strains of Microorganisms^{a,b}

no.	MIC of compd/MIC of TMP (1) ^c			
	S.a. CN 491	E.c. CN 314	S.t. CN 512	P.v. CN 329
1 (TMP)	1	1	1	1
3	>200	100	300	>100
4	20	1	1	>100
5	20	100	300	>100
6	2	300	>1000	>100
7	2	300	300	>100
8	1	100	500	>50
9	200	300	100	>100
12	6	30	30	>100
13	200	100	1000	>100
14	10	100	100	50
15	2	1000		>100
16	2	100	30	>100
17	0.2	100	50	>50
18	60	100	10	>100
21	6	1000	300	>100

^a Compounds 10, 11, 19, 20 were not tested. ^b Abbreviations: S.a., *Staphylococcus aureus*; E.c., *Escherichia coli*; S.t., *Salmonella typhosa*; P.v., *Proteus vulgaris*. ^c Values greater than 1 indicate activity less than that of TMP.

3 mM folic acid to the wash buffer. The active fractions were pooled and then dialyzed to remove folic acid. Overall yields ranged from 30–50%. Homogeneous enzyme from chicken liver was a gift from J. Freisheim, University of Cincinnati.

The *E. coli* enzyme was assayed in 0.1 M imidazole chloride, pH 7, and the rat and chicken liver enzymes were assayed in 0.05 M potassium phosphate, pH 7, by using method 1, previously described.³² I_{50} values were calculated as the concentration of free inhibitor required for a 50% decrease in velocity of the enzyme reaction. In all cases, reactions were initiated by the addition of dihydrofolate and the final, steady-state velocity was measured. For the weaker binding compounds 9–21, K_i values³⁶ were calculated with Cha's equation for competitive inhibitors.³⁷ The Henderson analysis,³⁸ as described by Baccanari and Joyner,²⁷ was used to determine *E. coli* enzyme K_i values for tight binding inhibitors. For each method values of multiple determinations

agreed within 15%. Equivalent K_i values were obtained from these two methods for TMP and several closely related analogues.

Relative binary K_D values of *E. coli* DHFR were determined as previously described³⁹ from competition experiments with MTX that were monitored by spectrophotometric analysis.

The in vitro antibacterial assays were carried out by Dr. L. Elwell and his staff using previously described methods.¹⁹

Crystallography. *Escherichia coli* (RT500) form 1 DHFR was prepared as described above and was crystallized from aqueous ethanol by vapor diffusion. Concentrations in the droplets at the start of the crystallization were as follows: enzyme (20 g/dm³), histidine hydrochloride buffer (pH 6.8, 50 mM in histidine), CaCl₂ (3.6 mM), compound 1 or analogue (2.5 mM), and EtOH (10% by volume). Reservoir EtOH concentration was in the range of 15–21%. Crystals were transferred to an aqueous medium containing EtOH (30%) and histidine hydrochloride buffer and CaCl₂ as above prior to X-ray measurement. Crystals grew in about 1 month and were hexagonal bipyramids, space group *P*6₁ with axial length of up to 1.2 mm. The unit cell dimensions ($a = b = 93.6$ Å, $c = 73.9$ Å) were similar whether crystals were grown in the presence of TMP or of an analogue.

The procedure for X-ray data collection and data processing and for the determination of the enzyme-TMP binary complex have been described.¹⁰ Isomorphous phases were calculated for 8563 native structure factors $F(\vec{h})$ of amplitude $F_{TE}(\vec{h})$ (TE = TMP-enzyme complex) to a spacing of 2.8 Å. A single-site uranium and a seven-site mercury derivative were used in phasing and the mean figure of merit was 0.635. The native map was calculated with Fourier coefficient amplitudes $m \cdot F_{TE}(\vec{h})$, where m was the figure of merit for $F(\vec{h})$. X-ray diffraction data to similar resolution were measured from crystals of compounds 4 and 7 and structure factor amplitudes F_{AE} (AE = analog-enzyme complex) were derived. Difference electron density maps between the analogue complex and the complex with TMP were calculated with $n \cdot m[F_{AE}(\vec{h}) - F_{TE}(\vec{h})]$ as Fourier coefficient amplitudes where n was 2 for acentric and 1 for centric reflections. This procedure placed the difference electron density map on a scale roughly compatible with that of the native map.⁴⁰ Combined maps, in which the difference maps were each added to the native map, were also calculated to image the respective analogue-enzyme complex.

The construction of a model of each of the two molecules of the complex of TMP and enzyme in the crystallographic asymmetric unit, using Kendrew skeletal components fitted to maps plotted on clear plastic at a scale of 2.0 cm Å⁻¹ and using a modified design of the optical comparator devised by Richards,⁴¹ has been described.¹⁰ In the fitting of models to electron density maps of the complexes containing compounds 4 and 7, the appropriate parts of the difference maps and the combined maps plotted on clear plastic were compared against the native map. The contouring levels on all maps were equivalent.

The root mean square error $\sigma(\rho)$ in electron density for difference maps was estimated by methods^{42,43} which roughly allow for the effects upon the electron density of random errors in the measurement of structure factor amplitudes, of errors in the isomorphous phases for the native structure, and of errors arising from the use of these phases alone rather than of phases appropriate to each complex. The estimates of error so obtained appeared fairly consistent with the general level of electron density fluctuation in the maps, features of magnitude $\geq 3\sigma(\rho)$ being very small and very sparse except in the region between the phenyl moiety of the analogues and Arg-57.

Acknowledgment. We thank Drs. David Henry and James Burchall for their encouragement and support of this work. Pauline Baker and Suzanne Joyner are gratefully acknowledged for their expert technical assistance, and we are indebted to Dr. Michael Cory and James

(36) The use of K_i values is the preferred method of representing inhibitor affinity, because it is a true kinetic constant, which at saturating NADPH equals the dissociation constant of I from the E-I-NADPH ternary complex. (Spector, T.; Cleland, W. W. *Biochem. Pharmacol.* 1981, 30, 1). The important factor to consider when comparing the relative binding of competitive inhibitors between two enzymes is that K_i values are independent of the Michaelis constant of the competing substrate whereas I_{50} values are not. For example, the ratio of rat liver and *E. coli* DHFR I_{50} values for TMP is approximately 53 000 ($37\,000 \times 10^{-6}$ M/ 0.7×10^{-6} M) under our assay conditions. However, mammalian dihydrofolate K_m values are commonly reported to be at least 10-fold lower than the *E. coli* value (Cha, S.; Kim, S. Y. R.; Kornstein, S. G.; Kantoff, P. W.; Kim, K. H.; Nagueb, F. N. M. *Biochem. Pharmacol.* 1981, 30, 1507). When a rat liver enzyme K_i for TMP is calculated from the I_{50} value (assuming a dihydrofolate K_m of 0.6 μ M), the ratio of rat liver and *E. coli* enzyme K_i values is less than 4000. Therefore, the I_{50} comparison overestimates the differential of TMP for the *E. coli* enzyme by a factor of about 10. Our attempts to determine a more precise dihydrofolate K_m value for the rat liver enzyme were hampered by nonlinear reactions at low substrate concentrations, where the velocities increased during the assay (data not shown). The mechanism of this anomaly was not investigated, but similar unexplained complex reaction kinetics have been observed with many other dihydrofolate reductases (ref 27). Therefore, although the I_{50} values in Table II are useful for comparing relative binding affinities of the inhibitors for the rat liver enzyme, they should not be used in an attempt to quantitate the degree of bacterial vs. mammalian enzyme specificity.

(37) Cha, S. *Biochem. Pharmacol.* 1975, 24, 2177.

(38) Henderson, P. J. F. *Biochem. J.* 1973, 135, 101.

(39) Dann, J. G. In "Chemistry and Biology of Pteridines"; Blair, J. A., Ed.; de Gruyter: New York, 1983; p 551.

(40) Luzzati, V. *Acta Crystallogr.* 1953, 6, 142.

(41) Richards, F. M. *J. Mol. Biol.* 1968, 37, 225.

(42) Beddell, C. R.; D. Phil. Thesis, Oxford, 1970.

(43) Blundell, T. L.; Johnson, L. N. "Protein Crystallography"; Academic Press: London, 1976; p 409.

Bentley for the implementation of NAMOD (Beppu, Y. *QCPE* 1979, 13, 370), the computer program used for producing the stereo drawings for this paper.

Registry No. 3, 82830-22-6; 4, 82830-23-7; 5, 82830-24-8; 6,

82830-25-9; 7, 82830-33-9; 8, 82830-26-0; 9, 78025-77-1; 10, 94236-24-5; 11, 94347-78-1; 12, 78025-89-5; 13, 82830-27-1; 14, 82830-28-2; 15, 82830-29-3; 16, 82830-30-6; 17, 82830-31-7; 18, 78025-76-0; 19, 94236-25-6; 20, 94236-26-7; 21, 78025-88-4; DHFR, 9002-03-0.

Synthesis and Dihydropteridine Reductase Inhibitory Effects of Potential Metabolites of the Neurotoxin 1-Methyl-4-phenyl-1,2,3,6-tetrahydropyridine

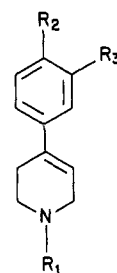
Wieslaw Gessner,^{†,§} Arnold Brossi,^{*†} Rong-sen Shen,[‡] and Creed W. Abell[‡]

Medicinal Chemistry Section, Laboratory of Chemistry, National Institute of Arthritis, Diabetes, and Digestive and Kidney Diseases, National Institutes of Health, Bethesda, Maryland 20205, and Department of Human Biological Chemistry and Genetics, Division of Biochemistry, The University of Texas Medical Branch, Galveston, Texas 77550. Received July 2, 1984

1-Methyl-4-phenyl-1,2,3,6-tetrahydropyridine (MPTP) is a nigrostriatal neurotoxin which can cause irreversible parkinsonism in humans and primates by selective destruction of neurons in the substantia nigra. It is possible that MPTP could be metabolized by hydroxylation of the phenyl ring and/or aromatization of its nitrogen-containing ring. Hydroxylated derivatives of 4-phenyl-1,2,3,6-tetrahydropyridine, 4-phenylpiperidine, and 4-phenylpyridine were synthesized and tested in vitro as inhibitors of dihydropteridine reductase (DHPR) from human liver and rat striatal synaptosomes. It was found that all hydroxy derivatives were about 100–10 000 times more inhibitory than MPTP to DHPR. The inhibitory potency of the hydroxylated derivatives increased with the number of hydroxyl substitutions present on the phenyl ring (catechol > phenol) and with oxidation of the nitrogen-containing ring (pyridine > tetrahydropyridine > piperidine).

It is well-known that 4-phenyl-4-(acyloxy)piperidine analgesics can be converted into 4-phenyl-1,2,3,6-tetrahydropyridines (TPYs) by hydrolysis¹ and dehydration¹⁻³ of the tertiary alcohols, chemically connecting these analgesics^{3,4} with tetrahydropyridines. 1-Methyl-4-phenyl-1,2,3,6-tetrahydropyridine (3, MPTP)³ and its analogues have been the subject of intense investigation in recent months because of reports that MPTP, a contaminant in an illegally manufactured drug,⁵ produced persistent parkinsonian symptoms in individuals who injected the crude drug⁵ and in a laboratory worker who was exposed to high levels of MPTP and its analogues.⁶ It was found that MPTP produces similar persistent pathological and neurochemical changes in rhesus monkeys⁷ but not in guinea pigs or rats.⁸ However, some investigators have recently observed neurotoxic effects of MPTP in rats^{9,10} and mice.¹¹ Given these results, it is intriguing to speculate whether the toxic effects of MPTP in humans might be related to the formation and/or clearance of metabolites.¹² Hydroxylation of the phenyl ring of 3, or aromatization of the heteromoiety, or both, could produce a series of metabolites of potential physiological importance.

In this paper we report an efficient synthesis of the catecholic TPYs 9 and 13, the piperidine analogues 19 and 21, and the pyridine 24, which is the most highly oxidized of the compounds prepared. The recent report that a quaternary 1-methyl-4-phenylpyridinium salt (MPP⁺) was found as the metabolite of 3¹³ prompted the preparation of the quaternary salts 25–28 for biological evaluation.



no.	R ₁	R ₂	R ₃
1	H	H	H
2	H	Cl	H
3	CH ₃	H	H
4	CH ₃	Cl	H
5	CH ₃	OH	H
6	CH ₃	OH	OCH ₃
7	H	OH	H
8	H	OH	OCH ₃
9	CH ₃	OH	OH
10	COCH ₃	OCOCH ₃	OCH ₃
11	COCH ₃	OH	OCH ₃
11a	CHO	OH	OCH ₃
12	COCH ₃	OH	OH
13	H	OH	OH
14	COCH ₃	OCH ₃	OCH ₃
15	H	OCH ₃	OCH ₃

At present, no simple model exists to evaluate the neurotoxic effects of such compounds. However, the ef-

[†] National Institutes of Health.

[‡] The University of Texas Medical Branch.

[§] Visiting scientist from A. Mickiewicz University, Poznan, Poland.

(1) Casey, A. F.; Beckett, A. H.; Iorio, M. A. *Tetrahedron* 1967, 23, 1405 and references cited therein.

(2) McElvain, S. M.; Berger, R. S. *J. Am. Chem. Soc.* 1955, 77, 2848.

(3) Ziering, A.; Berger, L.; Heineman, S. D.; Lee, J. *J. Org. Chem.* 1947, 12, 894.